

Dipole excitations of Ar substrate in contact with Na clusters

P. M. Dinh^{a*}, P.-G. Reinhard^b, E. Suraud^a

^aLaboratoire de Physique Théorique, Université Paul Sabatier, CNRS, F-31062 Toulouse Cédex, France

^bInstitut für Theoretische Physik, Universität Erlangen, D-91058 Erlangen, Germany

Abstract

We analyze the excitation of Ar substrate in contact with Na clusters using a previously developed hierarchical model for the description of the system constituted of a highly reactive metal cluster in contact with a rather inert substrate. Particular attention is paid to the dipole excitation of the Ar atoms and the energy stored therein. The Na clusters are considered at different charge states, anions, cations, and neutral clusters for the case of deposition and a highly ionized cluster embedded in a matrix. It is found that the dipole polarization of the Ar atoms stores the largest fraction of energy in the case of charged clusters. Some, although smaller, polarization is also observed for polar clusters, as Na₆. The effect is predominantly induced by the electrostatic interaction.

Key words: TDDFT, hierarchical approach, deposition dynamics, rare gas surface, dipole excitation

PACS: 31.15.ee, 31.70.Hq, 34.35.+a, 36.40.Wa, 61.46.Bc

1. Introduction

The study of clusters in contact with an environment has motivated many investigations over the years. Two major situations can be considered, namely a cluster deposited on a surface or a cluster embedded inside a matrix. Both situations bear some similarities and bring complementing information. Clusters on surfaces provide interesting perspectives for basic research and for applications to nano-structured materials [1,2], e.g., the synthesis of deposited clusters, either controlled growth of elementary units on a surface by molecular beam epitaxy [3] or direct deposition of size-selected clusters on a substrate [4]. One should also mention the non-destructive deposition technique of metal clusters on metal surfaces using a thin rare gas film above the metal surface [5]. At the side of embedded species, one can refer to the many studies exploring

the optical response in various dynamical scenarios [6,7,8] complementing similar investigations in the case of free clusters. Note furthermore that embedded clusters (or molecules) may also be viewed as model systems for a detailed analysis of radiation effects in matter [9,10].

From the theory side, the description of clusters in contact with an environment implies an extra complexity because one needs to account for the degrees of freedom of the substrate. Theoretical descriptions thus predominantly employ classical molecular dynamics with effective atom-atom forces, see [11]. This was, for example, done for the deposition dynamics of Cu clusters on metal [12] or Ar [13] surfaces, and of Al or Au clusters on SiO₂ [14]. Such simplified approaches overlook possible effects from electronic degrees of freedom which can become crucial in metal clusters, particularly if a finite net charge is involved. It is thus often necessary to account explicitly for electronic degrees of freedom. Fully detailed calculations have been performed which treat all

* Corresponding author

Email-address : dinh@irsamc.ups-tlse.fr

constituents with their electronic dynamics, e.g. for the structure of small Na clusters on NaCl [15] or the deposit dynamics of Pd clusters on a MgO substrate [16]. But the numerical effort of such detailed computations quickly grows huge. Furthermore, these subtle models are hardly extendable to truly dynamical situations, to larger clusters or substrates, and to systematic explorations for broad variations of conditions. This leaves space for a manifold of approximations allowing an affordable compromise between reliability and expense. Such methods are often called quantum-mechanical-molecular-mechanical (QM/MM) models and have been applied for instance to chromophores in biomolecules [17,18], surface physics [19,20], materials physics [21,22,23,24], embedded molecules [25] and ion channels of cell membranes [26]. We have developed such a QM/MM modeling, primarily in the case of Na in contact with Ar [27,28,29] and successfully applied this method to deposition dynamics on finite Ar clusters [30] or on Ar surfaces [31], as well as to irradiation scenarios in the case of embedded clusters both in the linear (optical response [32]) and non linear (hindered explosion [33,34]) domains. More recently, we have extended the modeling to a MgO substrate [35]. The originality of this approach lies in the fact that the environment polarizability is treated dynamically, a key aspect especially when charged species are considered [36].

In this paper, we want to further investigate the importance of this dynamical treatment of the environment's polarizability by exploring how the substrate's dipoles respond to a perturbation. We shall consider two typical scenarios : Cluster deposition on a surface and irradiation of an embedded cluster. In both cases, we shall explore in particular the impact of charge, either because the deposited species is charged, or because the embedded cluster acts as a chromophore in a laser field and thus quickly acquires charge after irradiation. This exploration is focused on theoretical aspects but is qualitatively closely related to recent experiments in which the deposition of charged Ag clusters on a Ar matrix, itself deposited on a Au surface has been studied [37,38]. It was shown in this experiment that the substrate, in spite of its a priori inert character, acquires a substantial inner excitation which plays a key role in the whole process. Exploring the dipole degrees of freedom in our Na-Ar combination then represents the simplest model case in relation to these experiments. We shall see that indeed, as suggested by our earlier investigations [36], these internal degrees of

freedom are readily excited in most of the studied cases.

The paper is organized as follows. After a brief reminder of the content of the model used here, we quickly focus on relevant test cases. We first show the overall importance of charge effects and then study the spatial extension of the inner excitation of the environment. We take examples from deposition processes and irradiation of embedded clusters.

2. Model

We first give a very brief summary of the hierarchical description of the combined Na-Ar system. We treat the metal atoms in full microscopic detail at the level of Time Dependent Local Density Approximation (TDLDA) for the valence electrons of the Na cluster. An average self-interaction correction is applied to LDA in order to put the ionization potential of the Na system at the correct place [39]. Electronic degrees of freedom are coupled to Molecular Dynamics (MD) for the ions. Details on this very successful TDLDA-MD approach for free clusters can be found in [40,41]. The environment (substrate or matrix) consists out of Ar atoms which are described by classical degrees of freedom, both in terms of position and dipole moment. The latter serves to take into account the dynamical polarizability of the substrate atoms. They have been adjusted carefully to recover the static and dynamical polarizabilities of Ar atoms. Electronic emission is not possible at the side of Ar atoms which limits the violence of the processes studied. But it is easy to check, in terms of the amplitude of Ar dipoles, how much energy is actually absorbed by an Ar atom. More precisely, this internal excitation energy of the Ar atoms is related, in our model, to the Ar dipole amplitude \mathbf{d} by

$$E_{\text{dip}} = \frac{1}{2} e^2 \frac{Q_{\text{Ar}}^2}{\alpha_{\text{Ar}}} \mathbf{d}^2, \quad (1)$$

where α_{Ar} is the static polarizability of bulk Ar, and Q_{Ar} the effective charge of the Ar cores [29].

As long as this energy (and correspondingly the dipole amplitude) remains safely below the Ar atom ionization potential, the model is perfectly applicable. We checked that this is always the case in all situations encountered here. For then, the dipole amplitude will represent the only possible inner excitation of Ar atoms. The Ar atoms are coupled to the Na by a long range polarization potential and some

short range repulsion to account for the Pauli blocking of cluster electrons in the vicinity of the Ar cores. The model has been calibrated to measured properties of typical Na-Ar systems. We refer the reader to [27,28,42] for a detailed description of the model and the detailed fitting of the various parameters.

In the case of deposition dynamics, the Ar(001) surface is modelled through an Ar₃₈₄ system, consisting in six layers of 8×8 Ar atoms with atoms in the two lowest layers frozen at bulk crystal positions. The layers are furthermore periodically repeated in both lateral directions, thus simulating bulk material in these two dimensions. We have checked that the finiteness of the sampling does not alter the results, at least qualitatively [30,36]. The dynamics is then initialized by placing the projectile at a finite distance (15 a₀) from the surface and boosting it with a given initial kinetic energy E_0 , towards the substrate and along the direction normal to it (denoted by z in the following). In the case of embedded species, the system is constructed by considering first a finite piece of bulk Ar, drilling a small hole in the center to insert the Na₈ cluster and then optimizing the whole ensemble (cluster + embedding material Ar₄₃₄) at the side of cluster electrons and ions and in terms of Ar positions and dipoles. The system is then irradiated by a laser and its response followed in time. We analyze the subsequent dynamics in terms of detailed ionic and atomic coordinates and dipoles.

3. Impact of charge

Let us first consider a typical example, namely the deposition of a Na₆⁺ cluster (consisting in a pentagon with a top ion on its symmetry axis) on Ar(001). We take a charged cluster in the spirit of [37,38] and a moderate initial kinetic energy in order to observe sticking of the cluster on the surface with no destruction of the substrate [31,43]. Fig. 1 shows the time evolution of positions and energies. In the upper panel are plotted the z -coordinates of ions (Na₆⁺) and surface (Ar) atoms. The z direction is the direction along the initial cluster velocity, perpendicular to the surface. The Na₆⁺ cluster is significantly perturbed as one can see from the large oscillations of the initially top ion going through the pentagon plane. Nonetheless, the overall process converges steadily to a robust sticking of the cluster on the surface. The surface itself is perturbed with some ionic rearrangement but with preservation of

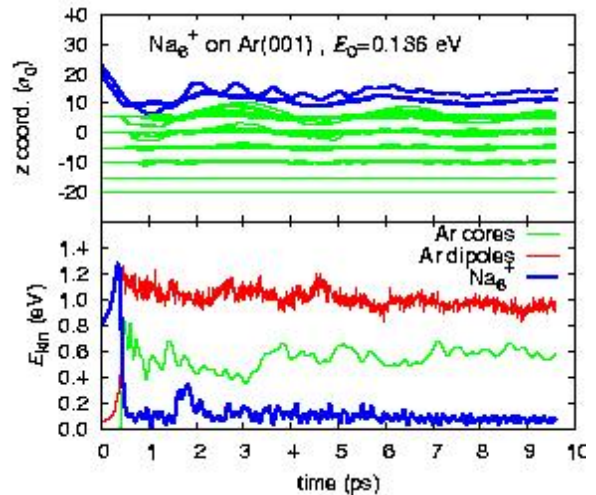


Fig. 1. Time evolution of coordinates and energies during dynamical deposition of Na₆⁺ on Ar(001) with initial kinetic energy $E_0 = 0.136$ eV/ion. Upper panel: z coordinates. Lower panel: total kinetic energy of Ar cores, Na ions and total dipole excitation energy.

layer structure. The lower panel of Fig. 1 displays the time evolution of energies, i.e. kinetic energies of cluster ions and Ar atoms, and the energy stored in Ar dipoles, see Eq. (1). The time evolution is rather simple with an almost instantaneous transfer of cluster kinetic energy to substrate degrees of freedom [30,31]. Note that some part of initial energy is flowing into potential energy which is not shown here. Still, the interesting feature is that, while Ar atoms acquire a significant kinetic energy of about half the maximum one of the cluster, they store about twice as much energy in their dipoles. This is a key aspect. It means that the substrate is not only heated up by cluster impact but also internally excited at the side of each constituent atom. This shows that a proper treatment of the dynamical surface polarizability can be crucial, particularly if a charge is involved. The energy sharing is established almost instantaneously at impact time and energies then remain rather constant in time.

The strong effect at the side of dipoles observed in Fig. 1 has to be explored further in order to try to identify where it comes from. Using a Na₆⁺ cluster as a projectile implies two possible effects, from charge and/or mass. We have considered here the case of a cationic cluster but an anionic one could be envisioned as well. We thus try to disentangle charge and mass effects by considering various possible combinations namely Na₆, Na₆⁺, Na₆⁻, Na, Na⁺ and Na⁻. We hence focus on dipole energies of the

six test cases, which are plotted as a function of time in Fig. 2. As compared to the Na_6^+ case, the dipole energies are suppressed by several orders of magnitude (2 for Na_6 and even 6 for Na) for neutral projectiles, while with charged projectiles, they are of the same order, with even a higher dipole energy for a positive charge by a factor about 1.5 with respect to the Ar core kinetic energies (not shown). The domi-

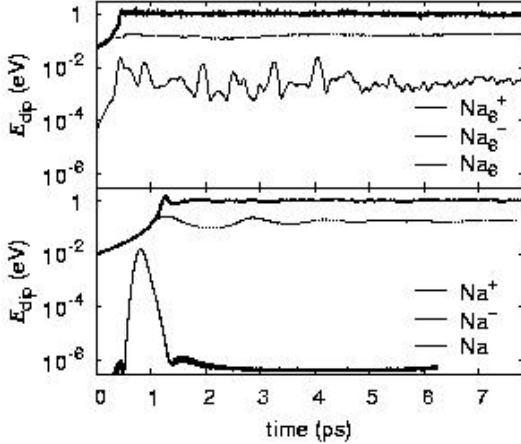


Fig. 2. Total excitation energy of the dipoles in the substrate Ar_{384} , after deposition of various metal species, as indicated, with initial kinetic energy $E_0 = 0.136$ eV/ion, as a function of time.

nant effect is obviously due to charge. In both mass cases (Na vs Na_6), the dipole energies associated to charged projectiles are several orders of magnitude larger than for the neutral cases. For neutral systems, one can spot a tiny mass effect by comparing Na to Na_6 but which, however, remains negligible with respect to charge effects. One also can notice a difference between anions and cations, the difference lying within one order of magnitude. The negatively charged electron cloud of the anions experience a stronger Pauli repulsion from the Ar cores. As a consequence, these projectiles cannot transfer as much energy to the Ar substrate as in the positively charged cases. This confirms earlier calculations on similar systems [36].

4. Details of energetics

From the previous section, we learnt that the matrix is qualitatively excited the same way either by Na^+ or Na_6^+ . To get more insight into the energetics, we present in this section the detail of the energy sharing for the case of deposition of Na^+ , which kicks

out the Ar atom just below the impact point and finally stays between the first and the second layers of the surface [36]. This case has the advantage that no valence electron contributes and that only one Na^+ ion is involved. Thus, there remain only five components to the total energy E_{tot} , namely

$$E_{\text{tot}} = E_{\text{pot}}^{\text{mat}} + E_{\text{dip}} + E_{\text{coupl}} + E_{\text{kin}}^{\text{Na}^+} + E_{\text{kin}}^{\text{mat}} \quad . \quad (2)$$

The kinetic energies are obvious. The contributions to the potential energy are: $E_{\text{pot}}^{\text{mat}}$ as the potential energy of the Ar matrix, consisting out of the Coulomb energy and a contribution from the Ar-Ar core repulsion, E_{dip} as the dipole excitation energy defined in Eq. (1), and E_{coupl} for the coupling energy between the Na^+ and the Ar matrix. As it should be, the total energy is well conserved during the deposition process (up to a relative error less than 0.01% over the whole simulation). Fig. 3 displays various terms

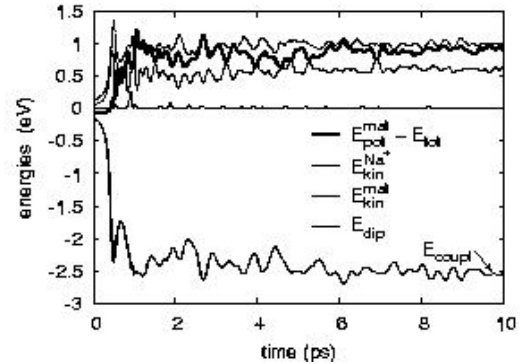


Fig. 3. Time evolution of the various contributions to the total energy as given in eq. (2) in the deposition of Na^+ on Ar_{384} , with respect to the total initial energy.

of Eq. (2) as a function of time. At initial time, the total energy E_{tot} of course consists of the initial Na^+ kinetic energy but mostly of the matrix potential energy $E_{\text{pot}}^{\text{mat}}$ (99.8 %) with small additional contributions from the coupling and dipole energies. These two latter contributions do not exactly vanish at initial time due to the initial finite distance at which the Na^+ ion is placed with respect to the Ar surface. Since the initial potential energy surface scales with the matrix size (hence with the finiteness of the representation of the surface), it makes little sense to keep it in the picture. We should hence remove it from the total energy (it is anyway a constant). But for sake of readability of Fig. 3, it appears simpler to remove the total initial energy $E_{\text{tot}}(t = 0)$ so that the components of the energy now sum up to zero at any time, as is clear from the figure. All contributions have a similar time structure. There is a fast

change within the first ps and then the values stabilize with some final fluctuations. The final share is the following : The largest and attractive contribution comes from the coupling energy. This is counterweighted to comparable parts between matrix potential energy, matrix kinetic energy, and dipole energy (still with the latter taking the lead) . The kinetic energy of the deposited Na^+ ion is negligible as it should be for a well bound particle.

It is also interesting to show the share of energies in relative units, we compare it with the total attachment energy of Na^+ to the surface which is $E_{\text{deposit}} = -4.7$ eV. Relative to the absolute value of that energy, we have the contributions :

$E_{\text{pot}}^{\text{mat}} - E_{\text{tot}}$	E_{coupl}	E_{dip}	$E_{\text{kin}}^{\text{Ar}}$	$E_{\text{kin}}^{\text{Na}}$
64%	56%	21.9%	13.7%	0.055%

The main contributions thus come from the potential energy due the rearrangement of the whole matrix, from the strong coupling between the Na^+ and the matrix (since the metal ion finally locates between the two first Ar layers), and from the internal excitation of each Ar atom.

5. Localization of the dipoles

The role of charge in the dipole energy suggests to explore in more detail the spatial distribution of the dipole excitation, with the intuition that it might resemble the response to a mere charge. We first present in Fig. 4 the dipole energies as a function of the axial coordinate $\rho = \sqrt{x+y}$ of the Ar cores, at impact time and only in the upper layer of the Ar substrate, for the case of the deposition of Na^+ with initial kinetic energy of 0.136 eV. The impact point is located at $\rho = 0$. We observe a high excitation of the dipoles which is strongly located around the impact point. As we shall see below, one does not observe any sizable evolution of this distribution, at least up to the times computed here, in terms of total dipole energies (see Figs. 1 and 2). In order to analyze this aspect in more detail, actual dipole moments (in fact, r.m.s. dipole moments $\bar{d} = \sqrt{d_x^2 + d_y^2 + d_z^2}$) as a function of time are plotted in Figs 5 (case of Na monomers) and 6 (case of Na_6 clusters). We discuss both cases simultaneously because they deliver very similar messages and because we have seen that mass effect is expectedly small. And yet, it is interesting to countercheck by comparing both, since the finite extension of Na_6 might influence the spatial distribution of Ar dipole excitations. In both figures are

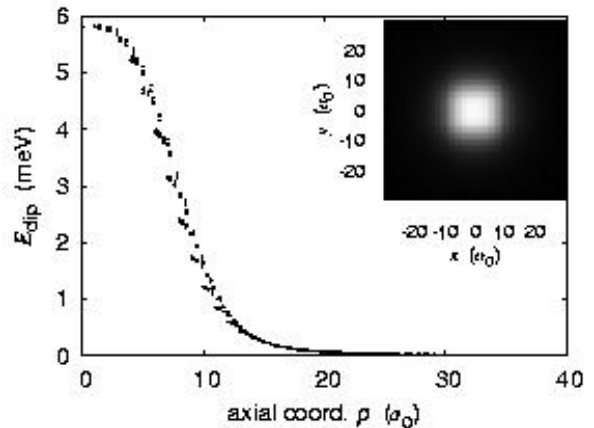


Fig. 4. Axial distribution of the dipole energies in the first layer of the Ar(001) substrate at impact time, for the deposition of Na^+ with initial kinetic energy $E_0 = 0.136$ eV. The insert shows a top view of the distribution in the first layer ($x - y$ plane).

plotted four snapshots corresponding to initial time, time of first impact and two later instants. There is obviously no significant time evolution of the distributions. One rather observes in Figs. 5 and 6 very similar pattern in both late times and both systems. One can spot differences in the neutral case; however the corresponding values are very small and one can probably ignore the point. Initial distributions as well are very similar in both figures, at least for charged clusters/atoms. The very regular trend is typical of a population of dipoles subject to a distant point charge, as is the case for initial states. The most interesting panels are probably the ones corresponding to impact time : One can note a significant perturbation of the distributions. This is especially true in the case of Na_6 , most probably because of its finite extension which perturbs the matrix on a larger range. The effect actually remains for longer times, with a somewhat (although not significantly) fuzzier distribution in the Na_6 case. The predominant effect is that finally the dipole excitations remain strongly located close to the cluster impact point. Everything thus looks as if the charge was simply put closer to the surface with the ensuing enhanced response of the dipole accompanied by a bit of “noise” at the distant points. In that respect, the details of the deposition dynamics are to a large extent irrelevant. Only charge and its localization are really important. This is in accordance with our previous study of neutral or charged Na monomer deposition/reflection on an Ar surface [36]. Indeed, as soon as the Na projectile is reflected, no sizable

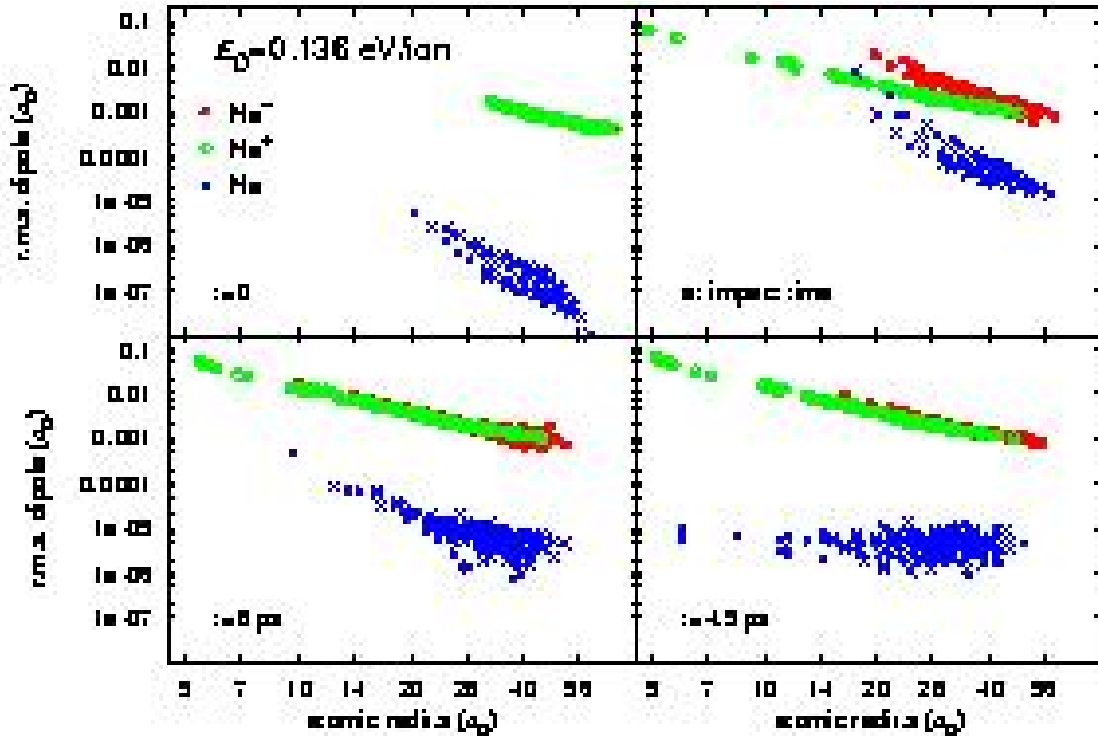


Fig. 5. Root mean square dipole moments of Ar atoms as function of Ar atomic radius, at four different times as indicated, for deposition with initial kinetic energy $E_0 = 0.136$ eV of Na, Na^+ and Na^- on Ar(001).

dipole energy beyond “noise” is left in the Ar substrate. Substantial dipole response is seen only at impact time, that is, when the (charged) projectile is sufficiently close to the Ar atoms. Thus, in these deposition processes, we are facing predominantly an electrostatic effect of the polarization of the surface. This effect is, however, energetically important and needs to be taken into account.

6. An example from embedded clusters

We have focused up to now on the case of cluster deposition. It is also interesting to study what occurs in the embedded case in which high charge states can be easily attained by laser excitation. We take as an example the irradiation of a Na_8 cluster embedded inside a finite Ar_{434} matrix. The laser pulse is kept short to concentrate the ionization to a fairly well defined initial time and the intensity is tuned such that the irradiation leaves the cluster with a net 3+ charge. A Coulomb explosion of the cluster is hindered by the matrix which stabilizes that high charge state, but allows a sizable oblate expansion of the cluster [33,34]. The point is illustrated in

the upper panel of Fig. 7 which shows the ionic and atomic positions along laser polarization axis as a function of time. The Ar matrix is also strongly perturbed with significant atomic rearrangement but the whole system finally remains stable. The lower panel of Fig. 7 displays energies: The kinetic energy of Na ions and Ar cores, and the energy stored in the Ar dipoles. The energy balance is to some extent incomplete as it misses the potential energy of cluster and matrix. But, as in case of deposition, the kinetic and dipole energies provide sufficient information about energy flow. We see in the lower part of Fig. 7 a behavior similar to the deposition case, namely that the initial Na motion is quickly damped and its energy accordingly transferred to the matrix. Again, one observes a significant amount of energy stored in the Ar dipoles, about three times as much as in the Ar core kinetic energy.

To complement the analysis of this irradiation case, we consider again the spatial distributions of dipoles at various instants in Fig. 8. The geometry is now a bit more complicated and we should care for both directions, along the laser polarization (z direction) and perpendicular (axial direction) to it. We thus slightly change the representa-

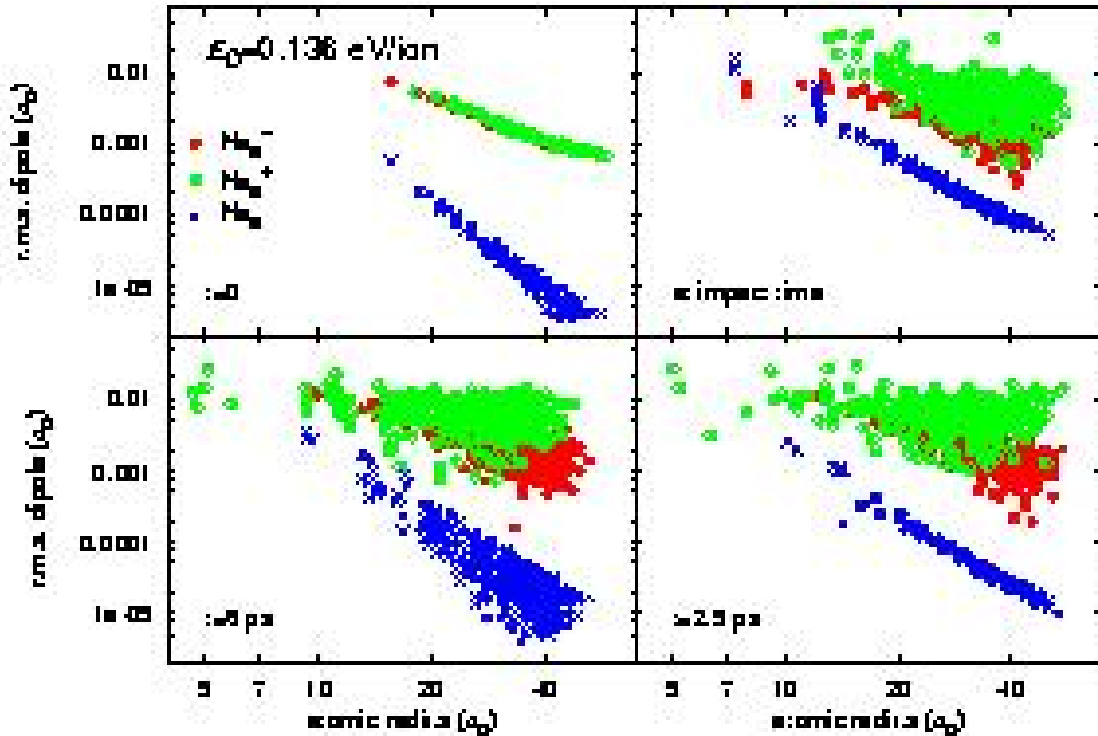


Fig. 6. Root mean square dipole moments of Ar atoms as function of Ar atomic radius, at four different times as indicated, for deposition with initial kinetic energy $E_0 = 0.136$ eV/ion of Na_6 , Na_6^+ and Na_6^- on Ar(001).

tion of the distribution in Fig. 8 considering separately both directions. The situation is also different from the charged deposition case to the extent that the cluster is initially neutral. This explains the rather "democratic" distribution of dipoles all over the matrix at initial time (upper panels). This confirms earlier findings on the role of Ar polarizabilities even in low energy phenomena such as optical response [29,32]. The initial dipole amplitudes are rather small as compared to the values which they acquire when the cluster becomes charged (mind the scales of upper and lower panels). The lower panels of Fig. 8 show large values of dipoles, comparable to deposition of charge clusters (see Figs. 5 and 6). The distribution, though, looks at first glance quite different from the deposition cases with a maximum at a finite distance from center rather (in radial coordinates, right lower panel) than a monotonously decreasing shape. The effect is in fact due to the finite (large) extension of the Na cluster after irradiation. Indeed, a sizable fraction of Ar sites are embedded in the Na cluster electron cloud and thus see a screened charge, whence the reduced dipole polarization. In order to exemplify the point, we have also plotted in Fig. 8 the actual position of the most

external Na ions and this makes the pattern clear, with an effect only along radial coordinate due to the oblate shape of the irradiated cluster [33,34]. Apart from that detail, we find again a dominantly static charge effect explaining the dipole polarizations of Ar atoms, much similar to the deposition case with localization prevailing again and little own dynamics.

7. Conclusion

We have discussed in this paper the atomic response of an Ar surface or matrix perturbed by a metal cluster either through deposition or irradiation by a laser. We have focused the analysis on the internal response of the Ar atoms by studying their single internal degree of freedom in our model, namely their dipole polarizability. We have seen that the dominant effect is due to cluster charge. Mass effects are mostly negligible with respect to charge effects. We have also analyzed how the dipole excitations are spatially distributed. We have observed that the excitation remains strongly localized and essentially does not evolve in time. It resembles in

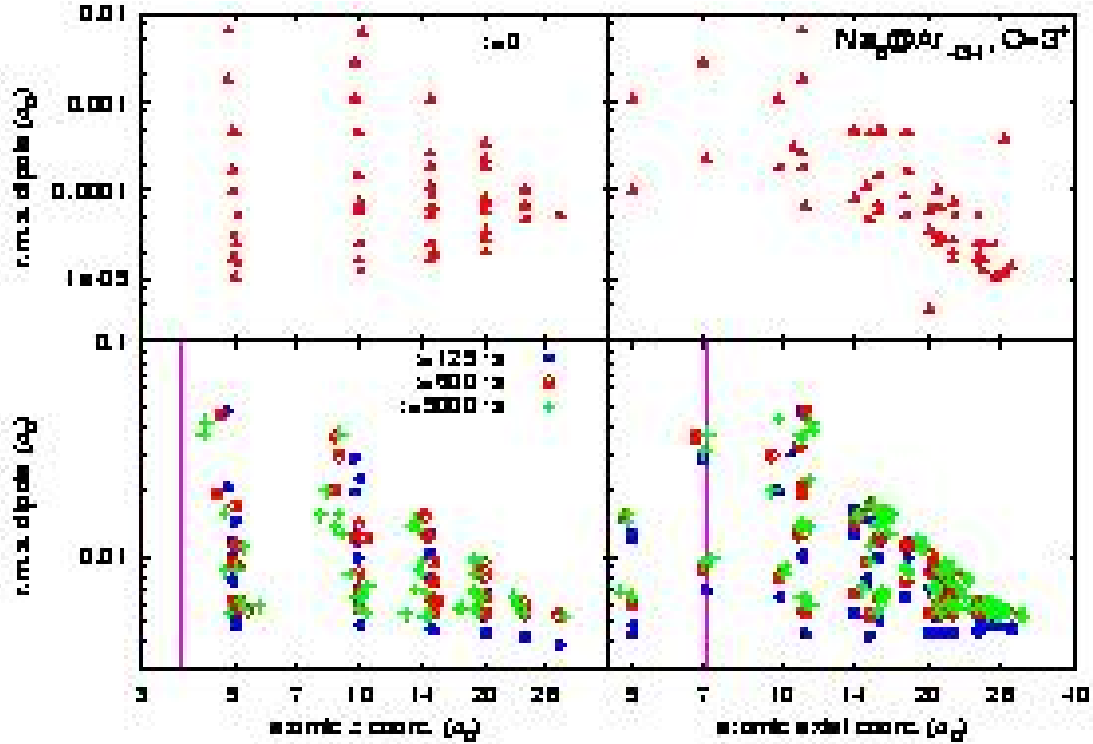


Fig. 8. Root mean square Ar dipoles for the hindered Coulomb explosion of Na_8 embedded in Ar_{434} , exposed to a laser of intensity $2 \times 10^{12} \text{ W/cm}^2$, frequency $\omega = 1.9 \text{ eV}$, and FWHM=33 fs. Left panel : Distribution as a function of the Ar z coordinates; right panels : That as a function of the Ar axial coordinates $\rho = \sqrt{x^2 + y^2}$. Top panels : At initial time; bottom panels : For three subsequent times as indicated. The maximum of excitation energy observed in the bottom right panel at $11 a_0$ is due to the oblate deformation of the created Na_8^{3+} . The vertical lines in the bottom panels indicate the corresponding coordinates of the outer Na_8 ions.

many respect the effect of a finite charge deposited at some place in the system. This holds true, up to details, for all situations involving charges, in deposition as well as in irradiation dynamics. Independent dynamical evolution of the Ar dipoles creates some background noise which, however, remains quantitatively unimportant at the present level of analysis. The quantitatively very important effect remains the nearly static dipole deformation. The Ar dipoles store a sizable fraction of the available energy. This is in perfect qualitative agreement with recent experiments on similar systems.

Acknowledgments : This work was supported by the DFG, project nr. RE 322/10-1, the French-German exchange program PROCOPE nr. 07523TE, the CNRS Programme “Matériaux” (CPR-ISMIR), Institut Universitaire de France, the Humboldt foundation, a Gay-Lussac price, and the French computational facilities CalMip (Calcul en Midi-Pyrénées), IDRIS and CINES.

References

- [1] H. Haberland, ed., *Clusters of Atoms and Molecules 2- Solvation and Chemistry of Free Clusters, and Embedded, Supported and Compressed Clusters*, vol. **56**, Springer Series in Chemical Physics, Berlin, 1994.
- [2] C. Binns, Surf. Sci. Rep. **44** (2001) 1.
- [3] H. Brune, *Metal Clusters at Surfaces, Structures*, Springer, Berlin, 2000.
- [4] W. Harbich, *Metal Clusters at Surfaces, Structures*, Springer, Berlin, 2000.
- [5] J. T. Lau, A. Achleitner, H. U. Ehrke, U. Langenbuch, M. Reif, W. Wurth, Rev. Sci. Instrum. **76** (2005) 063902.
- [6] W. Harbich, S. Fedigro, and J. Buttet, Z. Phys. D **26** (1993) 138.
- [7] M. Gaudry, J. Lermé, E. Cottancin, M. Pellarin, J-L Vialle, M Broyer, B Prével, M Treilleux, P. Mélinon, Phys. Rev. B **64** (2001) 085407.
- [8] T. Diederich, J. Tiggesbäumker, K.H. Meiwes-Broer, J. Chem. Phys. **116** (2002) 3263.
- [9] M. Barat, J. C. Brenot, J. A. Fayeton, Y. J. Picard, J. Chem. Phys. **117** (2002) 1497.
- [10] M. Y. Niv, M. Bargheer, R. B. Gerber, J. Chem. Phys. **113** (2000) 6660.

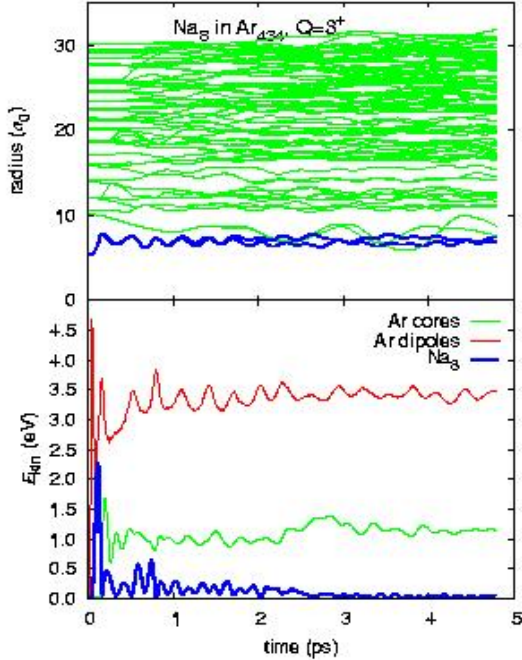


Fig. 7. Time evolution of radial coordinates $r = \sqrt{x^2 + y^2 + z^2}$ (upper panel) and kinetic energies (lower panel) for Na_3 excited by laser of intensity 2×10^{12} W/cm^2 , frequency $\omega = 1.9$ eV, and pulse length with full width at half maximum of 33 fs. The laser lifts the Na_3 within less than 100 fs into a charge state of $Q = 3^+$.

[11] C. Xirouchaki, R. E. Palmer, *Vacuum* **66** (2002) 167.
 [12] H.-P. Cheng, U. Landman, *J. Phys. Chem.* **98** (1994) 3527.
 [13] M. Ratner, W. Harbich, S. Fedrigo, *Phys. Rev. B* **60** (1999) 11730.
 [14] S. Takami, K. Suzuki, M. Kubo, A. Miyamoto, *J. of Nanoparticle Res.* **3** (2001) 213.
 [15] H. Häkkinen, M. Manninen, *J. Chem. Phys.* **105** (1996) 10565.
 [16] M. Moseler, H. Häkkinen, U. Landman, *Phys. Rev. Lett.* **89** (2002) 176103.
 [17] N. Gresh, D. R. Garmer, *J. Comp. Chem.* **17** (1996) 1481.
 [18] E. Tapavicza, I. Tavernelli, U. Rothlisberger, *Phys. Rev. Lett.* **98** (2007) 023001.
 [19] A. Nasluzov, K. Neyman, U. Birkenheuer, N. Rösch, *J. Chem. Phys.* **115** (2001) 17.
 [20] C. Imtama, L. V. Moskaleva, I. V. Yudanov, K. M. Neyman, N. Rösch, *Chem. Phys. Lett.* **417** (2006) 515.
 [21] A. Rubio, L. Serra, *Phys. Rev. B* **48** (1993) 18222.
 [22] L. I. Kurkina, O. V. Farberovich, *Phys. Rev. B* **54** (1996) 14791.
 [23] J. Lermé, B. Palpant, B. Prével, M. Pellarin, M. Treilleux, J. L. Vialle, A. Perez, M. Broyer, *Phys. Rev. Lett.* **80** (1998) 5105.
 [24] J. Lermé, *Eur. Phys. J. D* **10** (2000) 201.
 [25] M. Sulpizi, U. Röhrig, J. Hutter, U. Rothlisberger, *Int. J. Quantum Chem.* **101** (2005) 671.

[26] D. Bucher, S. Raugei, L. Guidoni, M. D. Peraro, U. Rothlisberger, P. Carloni, M. L. Klein, *Biophys. Chem.* **124** (2006) 292.
 [27] F. Dupl aa, F. Spiegelmann, *J. Chem. Phys.* **105** (1996) 1492.
 [28] B. Gervais, E. Giglio, E. Jaquet, A. Ipatov, P.-G. Reinhard, E. Suraud, *J. Chem. Phys.* **121** (2004) 8466.
 [29] F. Fehrer, P.-G. Reinhard, E. Suraud, E. Giglio, B. Gervais, A. Ipatov, *Appl. Phys. A* **82** (2005) 151.
 [30] P. M. Dinh, F. Fehrer, G. Bousquet, P.-G. Reinhard, E. Suraud, *Phys. Rev. A* **76** (2007) 043201.
 [31] P. M. Dinh, F. Fehrer, P.-G. Reinhard, E. Suraud, *Eur. Phys. J. D* **45** (2007) 415.
 [32] F. Fehrer, P. M. Dinh, P.-G. Reinhard, E. Suraud, *Phys. Rev. B* **75** (2007) 235418.
 [33] F. Fehrer, P. M. Dinh, P.-G. Reinhard, E. Suraud, *Eur. Phys. J. D* **45** (2007) 447.
 [34] F. Fehrer, P. M. Dinh, P.-G. Reinhard, E. Suraud, *Comp. Mat. Sci.* **42** (2008) 203.
 [35] M. B ar, L.V. Moskaleva, M. Winkler, P.G. Reinhard, N. R osch, E. Suraud, *Eur. Phys. J. D* **45** (2007) 507.
 [36] P. M. Dinh, F. Fehrer, P.-G. Reinhard, E. Suraud, *Surf. Sci.* **602** (2008) 2699.
 [37] C. Sieber, W. Harbich, K.H. Meiwes-Broer, C. F elix, *Chem. Phys. Lett.* **433** (2006) 32.
 [38] W. Harbich, Ch. Sieber, K.-H. Meiwes-Broer, and Ch. Felix, *Phys. Rev. B* **76** (2007) 104306
 [39] C. Legrand, E. Suraud, P.G. Reinhard, *J. Phys. B* **35** (2002) 1115.
 [40] F. Calvayrac, P.-G. Reinhard, E. Suraud, C. A. Ullrich, *Phys. Rep.* **337** (2000) 493.
 [41] P.-G. Reinhard, E. Suraud, *Introduction to Cluster Dynamics*, Wiley, New York, 2003.
 [42] F. Fehrer, P.-G. Reinhard, E. Suraud, *Appl. Phys. A* **82** (2006) 145.
 [43] P. M. Dinh, F. Fehrer, G. Bousquet, P.-G. Reinhard, E. Suraud, *Phys. Rev. A* **76** (2007) 043201.